

# Shear wave splitting in the Eastern Alps observed at the TRANSALP network

Jörn Kummerow\*, Rainer Kind

TRANSALP Working Group

*GeoForschungszentrum Potsdam, 14473 Potsdam, Germany*

Received 20 February 2005; received in revised form 9 July 2005; accepted 4 October 2005  
Available online 10 January 2006

## Abstract

Data from the temporary TRANSALP seismic network were analysed to investigate the seismic anisotropy in the upper mantle beneath the Eastern Alps. We operated mostly short period and some broadband stations in a dense linear array, which transects the Eastern Alps at  $\sim 12^\circ$  E longitude. Recorded SKS and SKKS phases with different backazimuths were used simultaneously to calculate the splitting parameters of delay time and fast axis direction for each seismic station. While we found variations in the delay times between  $\sim 0.8$  and  $2.0$  s, the determined fast axis directions prove to be rather consistent along the profile ( $60^\circ$ – $70^\circ$  N). They coincide well with the trend of the Eastern Alps, thus suggesting orogen-parallel flow in the upper mantle. Our findings support the earlier proposed idea that the Adriatic indenter which was forced northwards into the European plate during the late stage of the Alpine orogeny, triggered an escape movement to the less constrained Pannonian basin to the east.

© 2005 Elsevier B.V. All rights reserved.

*Keywords:* Anisotropy; Upper mantle; TRANSALP; Eastern alps

## 1. Introduction

The Alps are the result of convergence and collision between Europe and the Adriatic microplate since late Cretaceous time. During this process, European lower crust was thrust ESE/S under the more rigid Adriatic crust resulting in an asymmetric and complex architecture of the orogen. Based on steep angle reflection lines in the Western and Central Alps [*ECORP-CROP*, *NRP-20*, see Roure et al. (1996), and Pfiffner et al. (1997)], detailed models for the crustal structure and its evolution have been derived [e.g. (Schmid et al., 1996;

Schmid and Kissling, 2000)]. The recent combined reflection and receiver function TRANSALP profile has extended the high resolution image of the Alpine crust to the Eastern Alps (TRANSALP Working Group, 2001, 2002; Kummerow et al., 2004).

On the other hand, reliable geophysical information about the upper mantle beneath the Alps is rather scarce (Kissling, 1993). This is particularly true for the eastern part of the Alps. The best resolved parameter is seismic P-wave velocity, obtained from several regional tomography studies [e.g. (Spakman et al., 1993; Piromallo and Morelli, 2003; Lippitsch et al., 2003)]. They consistently indicate positive  $v_p$  anomalies down to some hundred kilometers depth, which are interpreted as southeastwards subducted European lower lithosphere

\* Corresponding author. Tel.: +49 331 288 1239.

E-mail address: [joern@gfz-potsdam.de](mailto:joern@gfz-potsdam.de) (J. Kummerow).

in the Western and Central Alps and northwards subducted Adriatic lower lithosphere in the Eastern Alps (Lippitsch et al., 2003). According to the Lippitsch et al. study, the location of the polarity reversal approximately concurs with the TRANSALP profile at  $\sim 12^\circ$  E. At the TRANSALP profile, however, we observed a south dipping subduction from receiver functions (Kummerow et al., 2004), more consistent with observations from the Western and Central Alps.

In this study, we determine the anisotropic properties of the upper mantle by measurements of SKS/SKKS shear wave splitting at the TRANSALP seismic stations in the Eastern Alps.

For almost two decades, the phenomenon of shear wave splitting has proven to be a reliable characteristic for azimuthal anisotropy in the upper mantle [e.g. Vinnik et al., 1984 (in Russian); Kind et al., 1985; Silver and Chan, 1988; Vinnik et al., 1989; Silver and

Chan, 1991]. Mantle anisotropy is commonly explained by strain-induced lattice preferred orientation (LPO) of olivine, with the fast axis aligning parallel to the mantle flow direction. In mountain belts, the orientation of the fast axis is often found to be sub-parallel to the strike of the main geological structures [e.g. (Vauchez and Nicolas, 1991; Vinnik et al., 1992; Silver, 1996; Barruol et al., 1998)], an observation, that documents the deep reaching deformation processes involved in the orogeny.

## 2. TRANSALP experiment and data

The TRANSALP seismic network was operated along a N–S profile corresponding to the TRANSALP seismic reflection transect at  $12^\circ$  E (TRANSALP Working Group, 2001 and Fig. 1). A distance of  $\sim 220$  km length was sampled, extending from the Molasse in

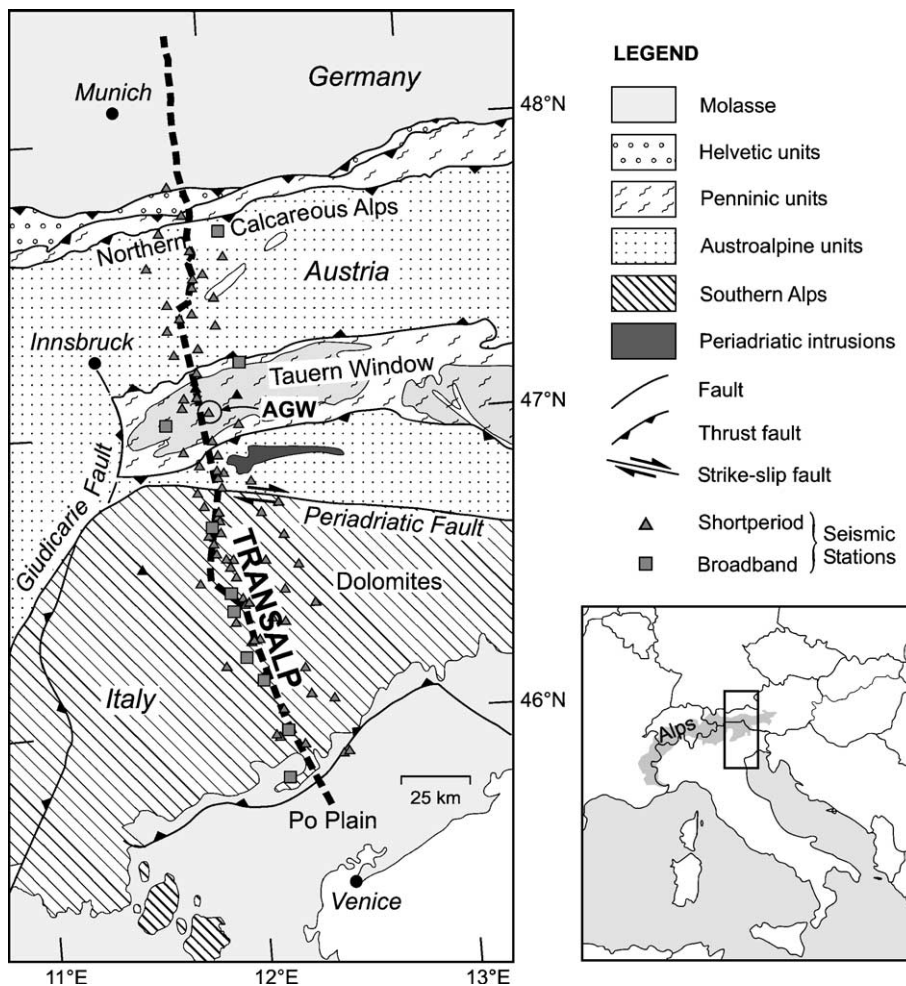


Fig. 1. Tectonic map and locations of the TRANSALP stations in the Eastern Alps. Data from station AGW are presented later in this study.

southern Germany through the Northern Calcareous Alps and Penninic units in Austria to the Southern Alps and the Po plain in northern Italy. On average 30 short-period (1 Hz), three-component and 3 broadband stations recorded continuously in two experiments from May 1998 to March 1999 and from August 1999 to October 1999. During the controlled source seismic campaign in September and October 1998, recordings from 20 additional three-component, short-period sensors were used. A supplementary experiment with 7 broadband instruments was initiated in the southern part of the profile in February 2002 and ended in November 2002 (Fig. 1). In this study we analyse data from total 36 SKS and SKKS events with epicentral distances between  $86^\circ$  and  $161^\circ$  and a relatively low signal to noise threshold ratio of 2, measured on the radial component (see Appendix A). The two core phases SKS and SKKS are particularly well qualified for anisotropy studies, since they ideally have a linear polarization in the radial plane due to the conversion from compressional to shear motion at the core mantle boundary. This is, of course, generally not the case for mantle S waves, where the polarization depends on the source properties. Since the angle of incidence at the surface is nearly vertical ( $\leq 10^\circ$ ) for SKS/SKKS waves, the horizontal resolution is good (about 50 km, depending on the wavelength of the SKS phase), while the vertical resolution of the anisotropic zone is very poor.

Due to the long periods of SKS phases, mantle anisotropy is commonly analysed with recordings from seismic broadband stations. In order to use our mostly short period data, we applied an instrument correction for the longer periods. As demonstrated in Fig. 2, this correction can be applied successfully to periods of at least 12 s. Examples of instrument-corrected and bandpass filtered seismogram sections of SKS/SKKS phases with different backazimuthal directions are shown in Fig. 3. Whereas there is no significant energy visible on the transverse components for two events (b and e in Fig. 3 with backazimuths  $67^\circ$  and  $248^\circ$  from N, respectively), all other events cause non-zero  $T$  amplitudes. Moreover, the average  $T$  trace is in all cases proportional to the time derivate of the average  $R$  trace. These two observations are strong indications for splitting of the incoming shear wave as a result of the existence of an anisotropic zone beneath the TRANSALP network (Kind et al., 1985). Data quality is low only for the event displayed in Fig. 4d (backazimuth  $201^\circ$  N), which represents the poorly sampled southern backazimuths.

### 3. Shear wave splitting analysis

We applied the multichannel analysis method by Chevrot (2000) to determine the splitting parameters delay time,  $\delta t$ , and direction of fast split wave,  $\phi$ . A

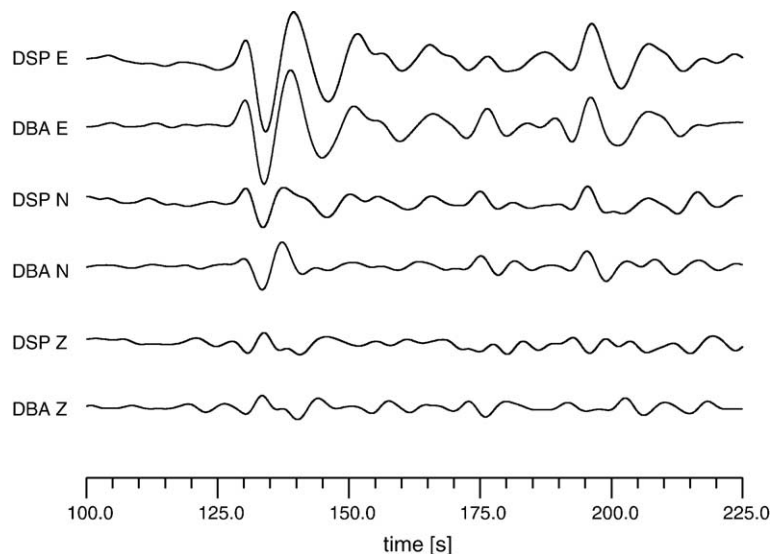


Fig. 2. Comparison of the three components E (east), N (north), and Z (vertical) recorded at a broadband station (DBA) with the traces, recorded at a close-by short-period station (DSP). The original short-period seismograms were instrument corrected to simulate broadband recordings. All traces are bandpass filtered between 5 and 12 s. The waveforms of the displayed SKS phase match well for all components. The distance between the two stations is  $< 2$  km.

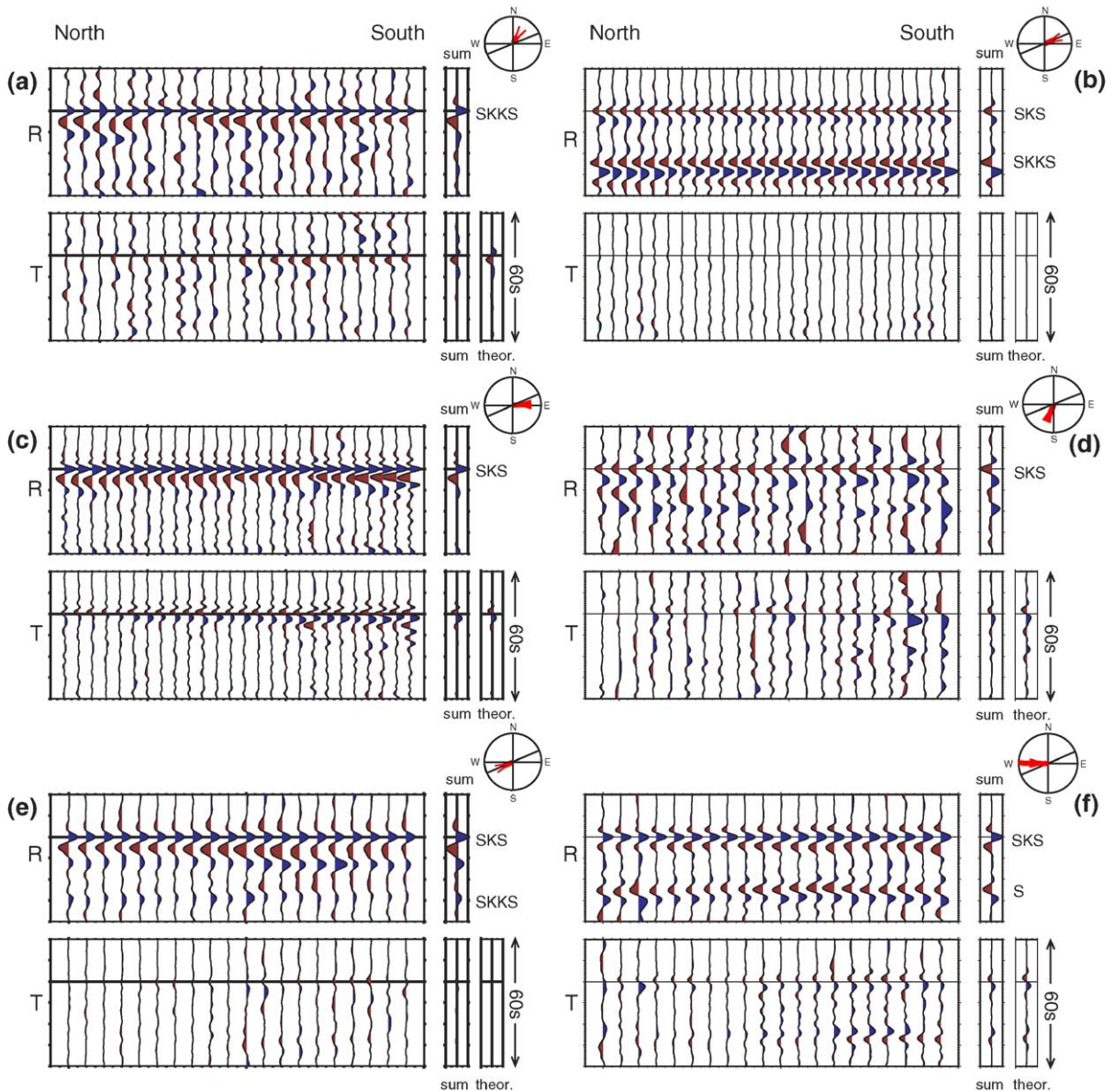


Fig. 3. Instrument corrected and 5–12 s bandpass filtered seismograms along the TRANSALP profile in the SKS/SKKS time window for 6 events with different backazimuths (a–f).  $R$  and  $T$  denote radial and transversal components. Radial directions are marked by arrows in the circle diagrams; the line represents the average fast axis and is oriented  $67^\circ$  N. The theoretical  $T$  components are calculated from the observed average  $R$  traces according to Eq. (2), assuming  $\delta t = 1.3$  s. Traces in each seismogram are sorted from north to south. A correlation between the traces for different events is not possible, since the station configuration was altered during the experiment.

transversely isotropic medium with horizontal axis of symmetry is assumed.

Using the approximate relation between radial ( $R$ ) and transverse ( $T$ ) component for an incoming wavelet  $\cos \omega t$  (with  $\omega \delta t \ll 1$ ), the components are given by

$$R(t) \approx \cos \omega t \quad (1)$$

$$T(t) \approx -0.5 \delta t \sin 2\beta R'(t) \quad (2)$$

(e.g. Vinnik et al., 1989).  $\beta$  is the angle between the fast axis and the radial axis. If the radial direction coincides with the fast axis ( $\beta = 0^\circ$ ) or the slow axis direction ( $\beta = 90^\circ$ ), the energy on  $T$  is minimal (no splitting occurs). For  $M$  events and  $N$  samples, Eqs. ((1),(2)) can be written as a  $M \times N$  tensor product

$$T = -0.5 \mathbf{s} \otimes r, \quad (3)$$

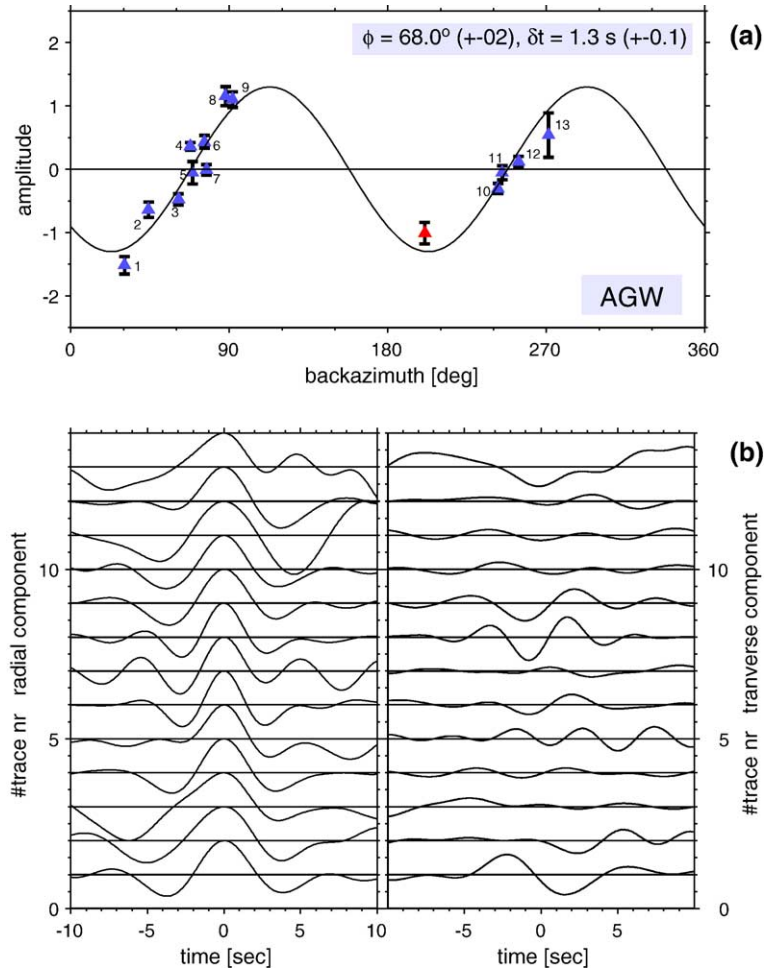


Fig. 4. Multichannel analysis of shear wave splitting applied to the data of TRANSALP station AGW. (a) Amplitude of the transverse component as a function of backazimuth, and the splitting function. (b) Normalized *R* and *T* traces for all recorded events, sorted for backazimuth. The event with a backazimuth of 201° N (red triangle) was only recorded at neighbouring stations and not at station AGW. It is shown here only to demonstrate its good fit with the sinusoid. The event was not included when calculating the splitting function. Numbers in (a) refer to the trace numbers in (b). (For interpretation of the references to colour in this figure legend, the reader is referred to the web version of this article.)

with the splitting vector  $\mathbf{s}$  and the radial component derivative  $r$  (after normalization, Chevrot (2000)).  $\mathbf{s}$  is given by

$$\mathbf{s} = -2 \frac{Tr}{\|r\|^2}, \quad (4)$$

and the splitting parameters  $\delta t$  and  $\phi$  can be determined by minimizing the penalty function

$$X^2 = \sum_{i=1}^M s_i - \delta t \sin(2\phi_i - 2\phi)^2, \quad (5)$$

where  $s_i$  and  $\phi_i$  are the splitting amplitude and backazimuth of event  $i$ , respectively (Chevrot, 2000, here for the case of a horizontal axis of symmetry). We solved Eq. (5) for optimal  $\delta t$  and  $\phi$  values by a grid-

search algorithm.  $\delta t$  depends both on the thickness of the anisotropic layer and the average coefficient of anisotropy.

We tested the routine with SKS data of the GRSN (German Regional Seismograph Network) seismic station FUR in Bavaria (southern Germany), which gives values of  $\phi = 60^\circ \pm 6^\circ$  and  $\delta t = 0.9 \pm 0.2$  s. The values are in good agreement with results published earlier by Vinnik et al. (1994) ( $\phi = 60^\circ$  and  $\delta t = 1.2$  s), although the delay time is slightly smaller.

The multichannel method is illustrated on the basis of the data of the TRANSALP station AGW, which is located in the Tauern Window in the central Eastern Alps (Fig. 1). The transverse components show, after normalization, a systematic variation with the backazimuth of the event (Fig. 4b). The clearest evidence of

shear wave splitting is given for traces 1 (backazimuth  $31^\circ$  N), 8 and 9 (backazimuths  $\sim 90^\circ$  N) with opposite signs of the  $T$  amplitude. All splitting amplitudes measured at station AGW can be fitted nicely by a sinusoid of period  $\pi$  (corresponding to a horizontal axis of symmetry, Fig. 4a). Delay time  $\delta t$  is read from the maximum amplitude of the sinus function and applying Eq. (2) ( $1.3 \pm 0.1$  s), and the axis orientation of the fast split wave from its phase ( $68 \pm 2^\circ$  N).

We consider all stations with more than 4 SKS and/or SKKS phases. Most stations have between 7 and 12 useful records. It is to note, that in comparison to the single-event techniques (e.g. Silver and Chan, 1991), the robustness of the multichannel method allows here

the splitting analysis of a by more than 50% increased amount of data. In this way, a better coverage of the backazimuthal range could be achieved. For example, we did not obtain reliable splitting parameters by the single-event method for the event from southern direction shown in Fig. 3c. The results are summarized in Fig. 5. The fast axis direction shows little variation along the profile ( $\phi \sim 60\text{--}70^\circ$  N) and small errors ( $< 5^\circ$ ). Values of  $\phi$  are slightly higher for stations located in the central part between  $\sim 47.4^\circ$  N and  $\sim 46.7^\circ$  N ( $\phi \approx 70^\circ$  N) and lower towards the northern and southern forelands ( $\phi \approx 60^\circ$  N, see Fig. 5c). The orientation is not only well constrained by shear wave splitting and energy on the  $T$  components, but also by the disappear-

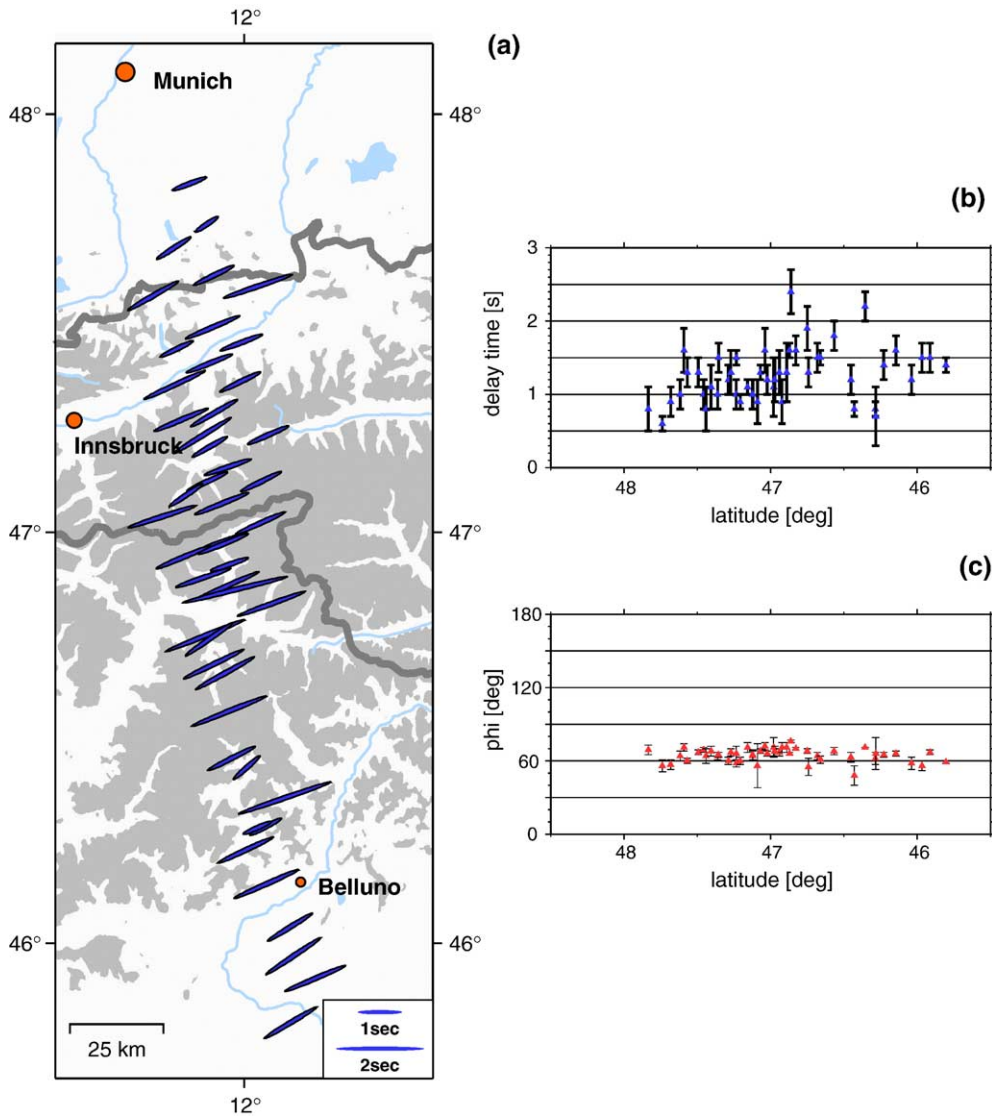


Fig. 5. Splitting parameters *delay time* and *direction of fast split wave* obtained by the multichannel analysis of TRANSALP stations with more than 4 recorded SKS/SKKS phases. The errors are given by the standard deviation.

ance of  $T$  energy in cases where the radial direction coincides with the fast axis direction (see Fig. 3, events b and e, and Fig. 4), and by the distinct slope of the sinusoid at zero-crossing. The delay time values are rather high (on average 1.3 s), but show considerable scatter ( $\sim 0.8$ – $2.0$  s) and errors ( $\sim 0.3$  s). We attribute this to the fact, that the azimuthal coverage is far from being homogeneous with gaps at  $95^\circ$ – $240^\circ$  and  $300^\circ$ – $30^\circ$  N. The amplitude minima and maxima of the sinusoid (at  $25^\circ$ ,  $205^\circ$  and  $115^\circ$ ,  $295^\circ$ , respectively) are not or only poorly sampled (Fig. 4 and Appendix A). This drawback is inherent to the location of the TRANSALP network relative to the global seismicity pattern.

Despite the scatter, there are some indications in our data, that the delay times  $\delta t$  increase southwards (Fig. 5b). They are smallest for the stations in the northern Molasse and the northern Calcareous Alps ( $\leq 1.0$  s); they reach values of  $\sim 1.0$ – $1.5$  s south of the Inn Valley and beneath the Tauern Window and are highest for stations south of the Tauern Window/Periadriatic Fault ( $\sim 1.5$  s). Our calculations are based on the assumption of a single anisotropic layer with a horizontal axis of symmetry. This simple model is supported by the observed splitting amplitudes, which can be well fitted by a sinus function of period  $\pi$  (Fig. 4). Due to the inhomogeneous azimuthal coverage, we cannot reliably distinguish from more complex scenarios such as a dipping axis or a multilayer

model, which would exhibit a different periodicity of the splitting amplitudes as a function of backazimuth. Considering that for western azimuths, the amplitudes of the splitting vector seem to be slightly weaker than for eastern azimuths (Fig. 4a), a dipping of the axis of symmetry towards W may be suspected.

#### 4. Interpretation/Conclusions

From analysis of shear wave splitting at seismic stations in Central Europe, Vinnik et al. (1994) postulated a relation of mantle anisotropy and the Alpine orogeny (see also Fig. 6). The splitting results at the TRANSALP stations also strongly suggest a coupling between measured anisotropy and the Alpine orogeny, with the fast direction being orientated roughly parallel to the trend of the Alps (in fact, it is orientated anticlockwise by  $\sim 10^\circ$  relative to the ridge of the Eastern Alps). This observation agrees with the sparse existing Pn anisotropy measurements in the Alps, which also show mountain-parallel fast axes (Smith and Ekström, 1999). The measured delay times of  $> 1$  s are too large to be explicable by a lower crustal effect alone. Based on the analysis of petrofabrics, Barruol and Mainprice (1993) derive a value of 0.1 s per 10 km. This results in a crustal contribution of maximum 0.3 s, a limit, which is broadly accepted. Hence, the major contribution must be derived

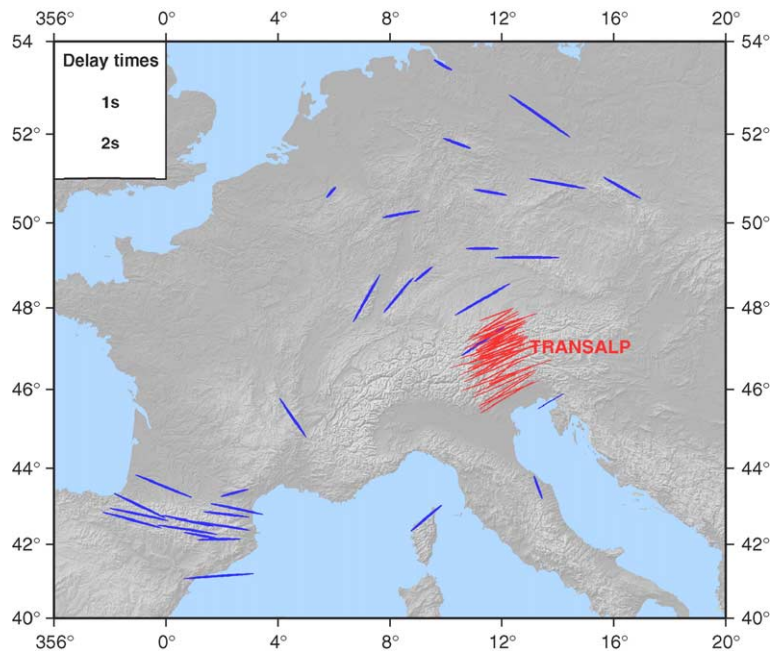


Fig. 6. Overview of splitting parameters for TRANSALP and other temporary and permanent seismic stations in central Europe. Data were compiled from previous publications (Bormann et al., 1993; Vinnik et al., 1994; Barruol and Souriau, 1995; Amato et al., 1998; Brechner et al., 1998; Granet et al., 1998; Wylegalla et al., 1999).

from the upper mantle. Meissner et al. (2002) proposed a lateral escape flow in the ductile lower crust and upper mantle beneath the Central and Eastern Alps towards the weaker Pannonian Basin in the east to explain the observed anisotropy. A similar concept of lateral extrusion was suggested by Ratschbacher et al. (1991) for the central part of the crust in the Eastern Alps based on structural geological evidence. Our TRANSALP splitting measurements indicate, that an escape is not restricted to the central part of the orogen, but encompasses a much broader zone of at least 200 km NS extent within the upper mantle. The thickness of the anisotropic zone can be estimated by assuming a value for the relative difference between slow and fast shear velocities,  $\delta V_s$ : For delay times  $\delta t \approx 1.0$ – $1.5$  s and  $\delta V_s$  values in the range of 2–4%, the resulting thickness is 150–300 km.

## Acknowledgments

We thank M. Savage and an anonymous reviewer for their constructive and careful reviews. This research was funded by the German Bundesministerium für Bildung und Forschung. Seismic stations of the TRANSALP experiment were provided by the station pool of the GFZ Potsdam, the University of Potsdam, the ETH Zürich, the University of Genova and the OGS Trieste. We like to thank R. Lippitsch for providing seismic data of part of the TRANSALP stations. Additional members of the TRANSALP Working Group are: H. Gebrande, E. Lueschen, M. Bopp, F. Bleibinhaus, M. Stiller, K. Millahn, H. Grassl, F. Neubauer, L. Bertelli, D. Borrini, R. Fantoni, C. Pessina, M. Stella, A. Castellarin, R. Nicolich, A. Mazotti, and F. Scherbaum.

## Appendix A. Events used for SKS/SKKS splitting analysis

No.	Date	Time	Latitude [°]	Longitude [°]	Depth [km]	Distance [°]	Magnitude	Backazi-muth [°]
1	1998/06/07	23:20:13.9	16.0	−93.8	87	88.8	6.3	292.2
2	1998/07/09	14:45:39.9	−30.4	−178.9	129	161.4	6.9	30.8
3	1998/07/24	18:44:04.4	21.3	122.0	33	87.5	6.1	61.3
4	1998/07/29	07:14:24.0	−32.3	−71.2	51	108.6	6.5	242.5
5	1998/08/04	18:59:20.1	−0.6	−80.4	33	92.1	7.1	271.3
6	1998/08/20	06:40:55.8	28.9	139.3	441	90.7	7.0	44.2
7	1998/09/02	08:37:29.9	5.4	126.7	50	102.5	6.8	67.9
8	1998/09/03	17:37:58.2	−29.4	−71.7	27	106.9	6.6	245.0
9	1998/09/22	01:16:55.4	11.8	143.1	9	107.0	6.0	50.5
10	1998/09/28	13:34:30.4	−8.2	112.4	152	103.0	6.6	88.0
11	1998/09/28	19:23:23.2	3.8	126.4	30	103.5	6.4	69.2
12	1998/10/08	04:51:42.8	−16.1	−71.4	136	97.2	6.2	254.2
13	1998/10/10	16:32:19.4	−0.4	119.8	33	102.4	6.0	77.1
14	1998/10/28	16:25:03.8	0.8	126.0	33	105.5	6.6	71.5
15	1998/11/29	14:10:31.9	−2.0	124.8	33	106.9	8.3	74.3
16	1998/12/06	00:47:13.4	1.2	126.1	33	105.3	6.6	71.1
17	1999/01/24	00:37:04.6	30.6	131.1	33	85.3	6.4	49.1
18	1999/02/23	07:27:56.4	0.2	119.5	33	101.7	6.2	76.9
19	1999/08/12	05:44:58.1	−1.7	122.4	28	105.1	6.1	75.9
20	1999/08/14	00:16:52.2	−5.8	104.7	101	96.0	6.4	92.0
21	1999/08/20	10:02:21.1	9.0	−84.2	20	87.6	6.9	280.6
22	1999/08/26	07:39:28.9	−3.5	145.6	33	121.0	6.6	57.5
23	1999/08/28	12:40:06.1	−1.2	−77.5	196	90.5	6.3	268.8
24	1999/09/15	03:01:24.3	−20.9	−67.2	218	98.0	6.4	248.0
25	1999/09/30	16:31:15.6	16.0	−96.9	60	90.8	7.5	294.5
26	1999/10/18	02:43:23.8	−56.1	−26.5	33	107.7	6.6	201.5
27	2002/03/28	04:56:22.4	−21.7	−68.3	125	99.2	6.1	248.3
28	2002/04/18	16:08:36.7	−27.5	−70.6	62	104.9	6.2	245.7
29	2002/05/26	00:10:21.0	1.8	127.2	109	105.6	5.8	69.8
30	2002/06/16	18:31:10.8	−2.3	102.6	231	92.1	5.8	91.2
31	2002/06/27	05:50:33.4	−7.0	103.9	10	96.3	6.5	93.4
32	2002/08/19	11:08:24.3	−23.9	178.5	675	154.5	7.0	29.8
33	2002/09/08	18:44:23.7	−3.3	142.9	13	119.3	6.5	59.9
34	2002/09/16	13:23:00.9	−3.3	142.7	10	119.2	5.9	60.1
35	2002/09/20	15:43:35.4	−1.7	134.2	10	112.7	5.9	66.4
36	2002/10/03	19:05:10.6	−7.4	115.8	315	104.8	6.0	85.0

Event information are taken from the USGS Preliminary Determination of Epicentres. Distances and azimuths are calculated for the centre of the TRANSALP line (47°N/12E).

## References

- Amato, A., Margheriti, L., Azzara, R., Basili, A., Chiarabba, C., Ciaccio, M., Cimini, G., Bona, M.D., Frepoli, A., Lucente, F., Nostro, C., Selvaggi, G., 1998. Passive seismology and deep structure in central Italy. *Pure Appl. Geophys.* 151, 479–493.
- Barruol, G., Mainprice, D., 1993. A quantitative evaluation of the contribution of crustal rocks to the shear wave splitting of teleseismic SKS waves. *Phys. Earth Planet. Inter.* 78, 281–300.
- Barruol, G., Souriau, A., 1993. Anisotropy beneath the Pyrenees range from teleseismic shear wave splitting. *Geophys. Res. Lett.* 22, 493–496.
- Barruol, G., Souriau, A., Vauchez, A., Diaz, J., Gallart, J., 1998. Lithospheric anisotropy beneath the Pyrenees from shear wave splitting. *J. Geophys. Res.* 103 (B12), 30039–30053.
- Bormann, P., Burghardt, P.-T., Makeyeva, L., Vinnik, L., 1993. Teleseismic shear-wave splitting and deformation in Central Europe. *Phys. Earth Planet. Inter.* 78, 157–166.
- Brechner, S., Klinge, K., Krüger, F., Plenefisch, T., 1998. Backazimuthal variations of splitting parameters of teleseismic SKS phases observed at the broadband stations in Germany. *Pure Appl. Geophys.* 151, 305–331.
- Chevrot, S., 2000. Multichannel analysis of shear wave splitting. *J. Geophys. Res.* 105 (B9), 21,579–21,590.
- Granet, M., Glahn, A., Achauer, U., 1998. Anisotropic measurements in the Rheingraben area and the French Massif Central: geodynamic implications. *Pure Appl. Geophys.* 151, 333–364.
- Kind, R., Kosarev, G., Makeyeva, L., Vinnik, L., 1985. Observations of laterally inhomogeneous anisotropy in the continental lithosphere. *Nature* 318, 358–361.
- Kissling, E., 1993. Deep structure of the Alps—what do we really know? *Phys. Earth Planet. Inter.* 79, 82–112.
- Kummerow, J., Kind, R., Oncken, O., Giese, P., Ryberg, T., Wylegalla, K., TRANSALP WORKING GROUP, 2004. A natural and controlled source seismic profile through the eastern alps: TRANSALP. *Earth Planet. Sci.*, 225. doi:10.1016/j.epsl.2004.05.040.
- Lippitsch, R., Kissling, E., Ansorge, J., 2003. Upper mantle structure beneath the alpine orogen from high-resolution teleseismic tomography. *J. Geophys.*, 108. doi:10.1029/2002JB002016.
- Meissner, R., Mooney, W.D., Artemieva, I., 2002. Seismic anisotropy and mantle creep in young orogens. *Geophys. J. Int.* 149, 1–14.
- Pfiffner, O., Lehner, P., Heitzmann, P., Mueller, S., Steck, A., 1997. Deep Structure of the Alps: Results from NRP 20. Birkhauser, Basel, Switzerland.
- Piromallo, C., Morelli, A., 2003. P-wave tomography of the mantle under the Alpine Mediterranean area. *J. Geophys.*, 108. doi:10.1029/2002JB00175.
- Ratschbacher, L., Frisch, W., Linzer, H., 1991. Lateral extrusion in the Eastern Alps: Part 2. Structural analysis. *Tectonics* 10 (2), 257–271.
- Roure, F., Bergerat, F., Damotte, B., Mugnier, J.-L., Polino, R., 1996. The ECORPS-CROP Alpine seismic traverse. *Mem. Geol. Fr.* 170 (113pp.).
- Schmid, S., Kissling, E., 2000. The arc of the western Alps in the light of geophysical data on deep crustal structure. *Tectonics* 19 (1), 62–85.
- Schmid, S., Pfiffner, O., Froitzheim, N., Schönborn, G., Kissling, E., 1996. Geophysical–geological transect and tectonic evolution of the Swiss–Italian Alps. *Tectonics* 15, 1036–1064.
- Silver, P.G., 1996. Seismic Anisotropy beneath the continents: probing the depths of geology. *Annu. Rev. Earth Planet. Sci.* 22, 385–432.
- Silver, P.G., Chan, W.W., 1988. Implications for continental structure and evolution from seismic anisotropy. *Nature* 335, 34–39.
- Silver, P.G., Chan, W.W., 1991. Shear wave splitting and sub-continental mantle deformation. *J. Geophys. Res.* 96 (B10), 16429–16454.
- Smith, G., Ekström, G., 1999. A global study of Pn anisotropy beneath continents. *J. Geophys. Res.* 104, 963–980.
- Spakman, W., van derLee, S., van der Hilst, R., 1993. Travel-time tomography of the European–Mediterranean mantle down to 1400 km. *Phys. Earth Planet. Inter.* 79, 3–74.
- TRANSALP Working Group, 2001. European orogenic processes research transects the Eastern Alps. *EOS, Trans. Am. Geophys. Union* 82, 453, 460–461.
- TRANSALP Working Group, 2002. First deep seismic reflection images of the Eastern Alps reveal giant crustal wedges and transcrustal ramps. *Geophys. Res. Lett.* 29 (10), 92–1–92–4. doi:10.1029/2002GL014911.
- Vauchez, A., Nicolas, A., 1991. Mountain building: strike-parallel motion and mantle anisotropy. *Tectonophysics* 185, 183–201.
- Vinnik, L.P., Kosarev, G., Makeyeva, L., 1984. Anisotropy of the lithosphere from observations of SKS and SKKS. *Dokl. Akad. Nauk SSSR* 278, 1335–1339. (in Russian).
- Vinnik, L.P., Kind, R., Kosarev, G.L., Makeyeva, L.I., 1989. Azimuthal anisotropy in the lithosphere from observations of long-period S-waves. *Geophys. J. Int.* 99, 549–559.
- Vinnik, L.P., Makeyeva, L., Milev, A., Usenko, A.Y., 1992. Global patterns of azimuthal anisotropy and deformations in the continental mantle. *Geophys. J. Int.* 111, 433–447.
- Vinnik, L., Krishna, V., Kind, R., Bormann, P., Stammer, K., 1994. Shear wave splitting in the records of the German Regional Seismic Network. *Geophys. Res. Lett.* 21 (6), 457–460.
- Wylegalla, K., Bock, G., Gossler, J., T.W. Group, 1999. Anisotropy across the Sorgenfrei–Torquist zone from shear wave splitting. *Tectonophysics* 314, 335–350.